

Contents lists available at ScienceDirect

# Biochemical and Biophysical Research Communications

journal homepage: www.elsevier.com/locate/ybbrc





# Spire2 and Rab11a synergistically activate myosin-5b motor function

Lin-Lin Yao a,b,1, Wei-Dong Hou b,b,1, Yi Liang a,b, Xiang-dong Li c,d, Huan-Hong Ji a,b,\*

- <sup>a</sup> School of Public Health, Jiangxi Medical College, Nanchang University, Nanchang, 330006, PR China
- <sup>b</sup> Jiangxi Provincial Key Laboratory of Preventive Medicine, Jiangxi Medical College, Nanchang University, Nanchang, 330006, PR China
- <sup>c</sup> Group of Cell Motility and Muscle Contraction, State Key Laboratory of Integrated Management of Insect Pests and Rodents, Institute of Zoology, Chinese Academy of Sciences, Beijing, 100101, PR China
- <sup>d</sup> University of Chinese Academy of Sciences, Beijing, 100049, PR China

## ARTICLE INFO

Keywords: Myosin-5b Spire2 Rab11a Synergistically activate Actin Vesicle transport

## ABSTRACT

Cellular vesicle long-distance transport along the cytoplasmic actin network has recently been uncovered in several cell systems. In metaphase mouse oocytes, the motor protein myosin-5b (Myo5b) and the actin nucleation factor Spire are recruited to the Rab11a-positive vesicle membrane, forming a ternary complex of Myo5b/Spire/Rab11a that drives the vesicle long-distance transport to the oocyte cortex. However, the mechanism underlying the intermolecular regulation of the Myo5b/Spire/Rab11a complex remains unknown. In this study, we expressed and purified Myo5b, Spire2, and Rab11a proteins, and performed ATPase activity measurements, pulldown and single-molecule motility assays. Our results demonstrate that both Spire2 and Rab11a are required to activate Myo5b motor activity under physiological ionic conditions. The GTBM fragment of Spire2 stimulates the ATPase activity of Myo5b, while Rab11a enhances this activation. This activation occurs by disrupting the head-tail interaction of Myo5b. Furthermore, at the single-molecule level, we observed that the GTBM fragment of Spire2 and Rab11a coordinate to stimulate the Myo5b motility activity. Based on our results, we propose that upon association with the vesicle membrane, Myo5b, Spire2 and Rab11a form a ternary complex, and the inhibited Myo5b is synergistically activated by Spire2 and Rab11a, thereby triggering the long-distance transport of vesicles.

# 1. Introduction

Intracellular vesicle transport is vital for cellular survival and fundamental function, and this process depends on the cytoskeleton, which comprises microtubules and actin filaments. Microtubules are rigid and extend radially throughout the cytoplasm. In contrast, actin filaments are short, dynamic and much less rigid than microtubules. Thus, microtubule and actin filaments are widely believed to serve as tracks for long-range and short-range vesicle transport, respectively. However, recent studies have shown that specific vesicles can be transported long-distance along actin tracks, rather than microtubules, through the coordination of vesicle-associated motors and track assembly proteins [1–5].

In mouse metaphase oocytes, Rab11a-positive vesicles are capable of long-range movement towards the oocyte cortex through a cytoplasmic

actin network. This network is assembled by the actin nucleation factors Spire and Formins at the vesicles, connecting the cytoplasmic vesicles to cell surface. Myosin-5b (Myo5b), a motor protein, associates with these vesicles, and drives them to move directionally along the actin network to reach the oocyte cortex [1,2,5]. Similarly, in melanocytes, melanosomes disperse over long-range centrifugally throughout the cell, depending on the cooperation of motor protein myosin-5a (Myo5a) and Spire/Formin at the organelle membrane [3,4]. However, little is known about how these proteins are coordinated in intracellular vesicle transport.

Myo5b, which serves as the motor center at the Rab11a-positive vesicles in mouse oocytes, can convert chemical ATP energy into mechanical force and move processively on actin filaments [6,7]. Myo5b structurally contains four distinct regions: the N-terminal motor domain (the head), the adjacent lever arm containing six IQ motifs (the neck

Abbreviations: Myo5b, Myosin-5b; HMM, heavy meromyosin fragment of Myo5b; CaM, calmodulin; GTD, globular tail domain of Myo5b.

<sup>\*</sup> Corresponding author. Department of Occupational Health and Toxicology, School of Public Health, Nanchang University, No. 461 Ba Yi Avenue, Nanchang, Jiangxi, 330006, PR China

E-mail address: jijian312@126.com (H.-H. Ji).

 $<sup>^{1}\,</sup>$  These authors contributed equally to this work.

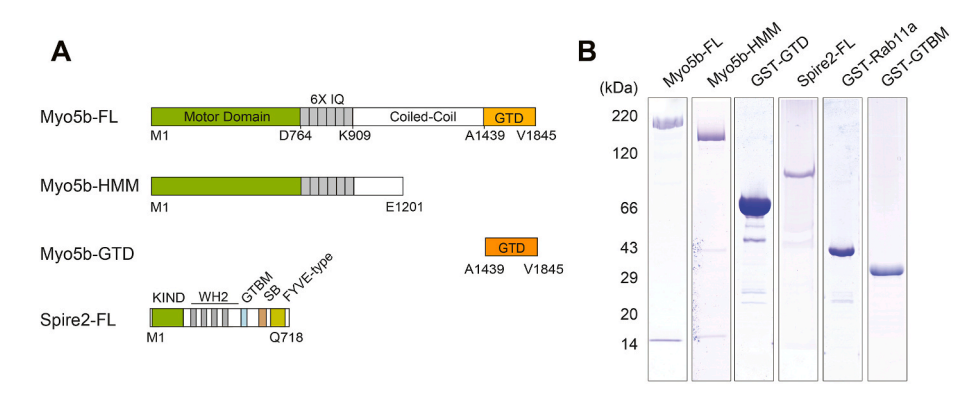


Fig. 1. Myo5b and its binding partners used in this study. (A) Schematic primary structure of Myo5b constructs and Spire2. Myo5b-FL, the full-length Myo5b; Myo5b-HMM, Myo5b truncation as indicated; Myo5b-GTD, the C terminal globular tail domain of Myo5b; Spire2-FL, the full-length Spire2. For clarity, the diagram was not drawn to scale. (B) SDS-PAGE (4–20%) of purified Myo5b and its binding partner proteins in this paper. FLAG-tagged proteins (Myo5b-FL, HMM and Spire2-FL) and GST-tagged proteins (Myo5b-GTD, Rab11a, and Spire2-GTBM) were expressed in Sf9 and BL21(DE3) *E. coli* cells, respectively.

region), a coiled-coil dimerization region in the middle, and the C-terminal globular tail domain (GTD) (Fig. 1A) [8–11]. The motor domain contains the nucleotide and actin filament binding sites, and can convert the energy of ATP hydrolysis into mechanical power to move along actin filaments. The coiled-coil region and the GTD domain recognize cargo or cargo adaptors [10,12]. Additionally, the GTD, composed of two closely apposed subdomains (subdomain-1 and subdomain-2), functions as an inhibitory domain by interacting with the N-terminal motor domain to prevent energy waste [8–15].

As an actin nucleation factor at the vesicle membrane, Spire consists of an N-terminal kinase-like non-catalytic domain (KIND) and four Wiskott-Aldrich syndrome protein homology 2 (WH2) domains that bind actin, followed by a Spire box (SB), and a C-terminal FYVE-type zinc finger domain that interacts with negatively charged membrane lipids (Fig. 1A) [16,17]. *In vitro* protein interaction assays have demonstrated that Spire proteins interact directly with Myo5b-GTD through a short conserved motif of 27 amino acids (Spire-GTBM), which is located between the WH2 domain and SB domain (Fig. 1A) [18]. Structural evidence indicates that Spire-GTBM binds to the subdomain-1 of the homologous Myosin5a (Myo5a) GTD, while Rab11a binds to subdomain-2, indicating that Myo5b/Spire2/Rab11a can form a ternary complex [18]. However, a critical question of how the molecules, especially Myo5b, are regulated in this complex remains unknown.

In this study, we expressed and purified Myo5b and its associated proteins, and performed ATPase activity measurements, pulldown and single-molecule motility assays. Our data demonstrate that both Spire2 and Rab11a are required to activate Myo5b motor function, indicating that precise intermolecular regulation exists in the Myo5b/Spire2/Rab11a complex during actin dependent long-distance vesicle transport.

# 2. Materials and methods

# 2.1. Materials

Q5 high-fidelity DNA polymerase and restriction enzymes were purchased from New England BioLabs (Beverly, MA). Oligonucleotides were synthesized by Sangon (Shanghai, China). Anti-FLAG M2 affinity sepharose, 2,4-dinitrophenyl-hydrazine, phosphoenolpyruvate (PEP), pyruvate kinase were purchased from Sigma-Aldrich (St. Louis, MO). FLAG (DYKDDDDK) peptide was synthesized by Augct (Beijing, China). Glutathione Sepharose 4 Fast Flow (GSH-Sepharose) was purchased from Solarbio (Beijing, China). Actin was prepared from rabbit skeletal muscle [19].

# 2.2. Cloning, expression and purification of Myo5b constructs and associated proteins

FLAG-tagged rat Myo5b full length and HMM (heavy meromyosin) fragment were prepared as previously described [15]. The cDNA of full-length Spire2 was synthesized by genewiz (Suzhou, China). To express Spire2 protein in Sf9 insect cells, the cDNA was subcloned into pFastBac vector and its recombinant baculovirus was generated using the Bac-To-Bac system (Invitrogen). Spire2 protein was expressed in Sf9 insect cells, and purified using anti-FLAG M2 affinity sepharose [20,21]. All clones mentioned in this paper were confirmed by DNA sequencing. The light chain of Myo5b, calmodulin (CaM), was prepared as previously described [22].

The cDNAs of Myo5b-GTD (comprising the C-terminal 407 residues of Myo5b), Rab11a, and Spire2-GTBM (residues 406–430 of Spire2) derived from PCR, were subcloned into pGEX4T1 vector, and expressed in *Escherichia coli* BL21(DE3). The GST-tagged Myo5b-GTD, Rab11a, and Spire2-GTBM proteins were further purified using GSH affinity chromatography following the standard procedures. The purified proteins were dialyzed against Dialysis Buffer (10 mM Tris-HCl (pH 7.5), 0.2 M NaCl and 1 mM DTT), and the concentrations were determined based on the absorbance at 280 nm using the following molar extinction coefficients (liters mol $^{-1}$ ·cm $^{-1}$ ): 74910 (GST-GTD), 63020 (GST-Rab11a), 41160 (GST-Spire2-GTBM). Activated Rab11a (GTP $\gamma$ S-Rab11a) was prepared by incubated with a 5-fold excess of GTP $\gamma$ S and MgCl $_2$  at 25 °C for 30 min.

# 2.3. ATPase assay

The ATPase activity of Myo5b was measured using an ATP regeneration system at 25  $^{\circ}\text{C}$  as described previously [23]. Unless otherwise indicated, the activity was measured in a solution containing 20 mM MOPS-KOH (pH7.0), 1 mM MgCl<sub>2</sub>, 200 mM KCl, 0.25 mg/ml BSA, approximately 60–100 nM Myo5b, 40  $\mu\text{M}$  actin, 12  $\mu\text{M}$  CaM, 1 mM EGTA, 0.5 mM ATP, 20 U/ml pyruvate kinase, 2.5 mM PEP, 1 mM DTT, and indicated concentrations of adaptor proteins.

# 2.4. Anti-FLAG pulldown assay

Anti-FLAG pulldown of FLAG-tagged Myo5b-HMM with GST-tagged GTD in the presence or absence of adaptor proteins was performed as follows. 18  $\mu l$  Anti-Flag M2 Sepharose beads were mixed with 100  $\mu l$  of 0.6  $\mu M$  Myo5b–HMM, 1.8  $\mu M$  GTD and 2.4  $\mu M$  GTP $\gamma S$ -Rab11a or 2.4  $\mu M$  Spire-GTBM in Reaction Buffer (20 mM MOPS-KOH (pH 7.0), 100 mM NaCl, 10  $\mu M$  CaM, 1 mM MgCl $_2$ , 3  $\mu M$  GTP $\gamma S$ , 1 mM EGTA, 1 mM DTT), and rotated at 4  $^{\circ} C$  for 2 h. The beads were then washed 4-5 times with 100  $\mu l$  of Wash Buffer (20 mM MOPS-KOH (pH 7.0), 50 mM NaCl, 1 mM

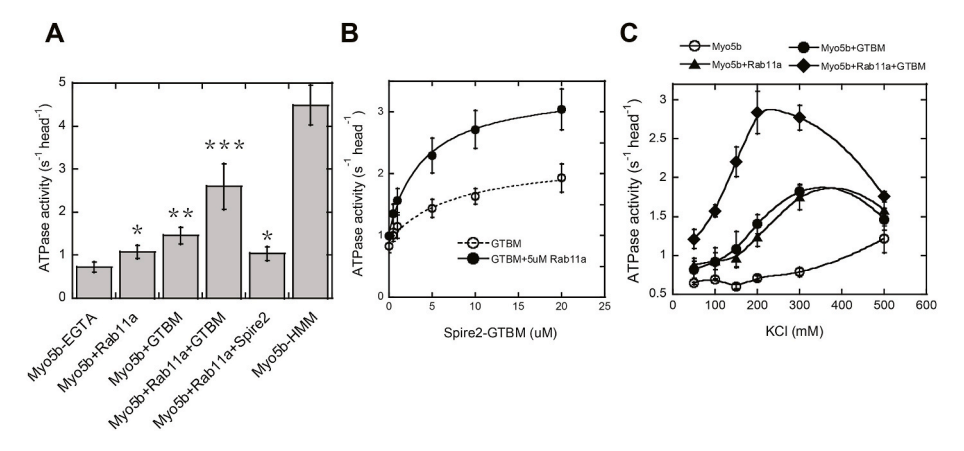


Fig. 2. The ATPase activity of Myo5b was co-activated by Spire2-GTBM and Rab11a. (A) The ATPase activity of Myo5b in the presence of Spire2 and Rab11a. The activity was measured in the presence of 8 μM Spire2 or Rab11a under the following conditions: 20 mM MOPS-KOH (pH 7.0), 200 mM KCl, 1 mM DTT, 1 mM MgCl<sub>2</sub>, 0.25 mg/ml BSA, 2.5 mM PEP, 20 units/ml pyruvate kinase, 12 μM CaM, 0.5 mM ATP, 40 μM actin, and 1 mM EGTA. Values are mean  $\pm$  S.D. from 3 to 4 independent assays. Asterisks (\*, P < 0.05; \*\*\*, P < 0.01; \*\*\*\*, P < 0.001) denote a statistically significant difference compared with the first column. The activity of Myo5b-HMM was included as a positive control. (B) The ATPase activity of Myo5b was activated by 0–20 μM Spire2-GTBM in the absence (open circles) or presence (closed circles) of 5 μM Rab11a. The activity was measured as described above, and fitted with a hyperbolic equation:  $V=V_0+V_{max}*$  [GTBM]/( $K_d+$  [GTBM]), where  $V_0$ , the ATPase activity in the absence of GTBM;  $V_{max}$ , the maximal activated ATPase activity; and  $K_d$ , the concentration of GTBM that simulates the ATPase activity to 50% of  $V_{max}$ . Values are mean  $\pm$  S.D. from three independent assays. (C) The effect of ionic strength on the activation of Myo5b ATPase activity by Spire2-GTBM and Rab11a. The ATPase activity of Myo5b was determined under EGTA conditions and 50–500 mM KCl in the absence or presence of 8 μM Spire2-GTBM and/or 10 μM Rab11a; closed squares, in the presence of 8 μM Spire2-GTBM and Rab11a; closed circles, in the presence of 8 μM Spire2-GTBM; closed triangle, in the presence of 10 μM Rab11a; closed squares, in the presence of 8 μM Spire2-GTBM and 10 μM Rab11a. All data are mean  $\pm$  S.D. from three independent assays.

MgCl<sub>2</sub>, 1  $\mu$ M GTP $\gamma$ S, 1 mM EGTA, 1 mM DTT). The proteins bound to the beads were eluted with 30  $\mu$ l of Elution Buffer (20 mM MOPS-KOH (pH 7.0), 200 mM NaCl, 0.2 mg/ml FLAG peptide, 1  $\mu$ M GTP $\gamma$ S, 1 mM MgCl<sub>2</sub>, 1 mM EGTA, 1 mM DTT). The eluted proteins were separated by regular SDS-PAGE (4–20%) and stained with Coomassie Brilliant Blue (CBB). The amounts of the Myo5b-HMM and GTD were quantified by NIH Image J software (Bethesda, MD).

# 2.5. Single-molecule motility assay

The in vitro single-molecule motility was performed at room temperature with slight modifications [24,25]. Approximately 10 µl volume of a flow chamber was assembled, and then fluxed with 30 µl of High Salt Buffer (10 mM Hepes-KOH (pH 7.5), 500 mM KCl, and 5 mM MgCl<sub>2</sub>). The chamber was incubated with 18 µl of 0.4 mg/ml N-ethylmaleimide-treated myosin in High Salt Buffer for 6 min, and then blocked with 15  $\mu$ l 1 mg/ml casein for 3 min. 10  $\mu$ l of 10 nM Alexa 488-phalloidin-labeled actin filaments in Low Salt Buffer (20 mM Hepes-KOH (pH 7.6), 25 mM KCl, 2 mM MgCl<sub>2</sub>, and 1 mM EGTA) were flowed into the chamber, and incubated for 3 min. The chamber was then rinsed with 35 µl of Low Salt Buffer containing 0.10 mg/ml casein, 40 units/ml glucose oxidase, 2000 units/ml catalase, and 1% glucose. Ultimately, the chamber was perfused with 30 µl of Reaction Solution (~1 nM Cy3B-labeled Myo5b, 10  $\mu M$  ATP, 10  $\mu M$  CaM, 40 units/ml glucose oxidase, 2000 units/ml catalase, 1% glucose,  $0.5\,\text{mM}$  PEP, and  $2\,$ units/ml pyruvate kinase in the presence/absence of 5  $\mu M$ GTPγS-Rab11a and/or 1 μM Spire2-GTBM in Low Salt Buffer).

Imaging was conducted at a frame rate of 5 s $^{-1}$  under an inverted total internal reflection fluorescence (TIRF) microscope (Nikon Ti-E) as described previously [26]. Images were analyzed and the number of Cy3B-labeled Myo5b that moved along actin filaments was quantified and normalized to the total length of actin filaments using NIH ImageJ software. Cy3B-labeled Myo5b, Alexa 488–phalloidin labeled actin filaments and N-ethylmaleimide-treated myosin were prepared as described previously [22,26,27].

# 2.6. Statistical analyses

All values are shown as mean  $\pm$  S.D. An unpaired Student's t-test was

used for statistical analysis, with significance defined as P < 0.05 (\*, P < 0.05; \*\*, P < 0.01; \*\*\*, P < 0.001) (GraphPad Prism software version 6.0 for Windows).

#### 3. Results

# 3.1. Spire2 and Rab11a collaboratively activate the ATPase activity of Myo5b

To investigate the impact of vesicle adaptors on Myo5b motor function, we prepared full-length and truncated Myo5b proteins, together with Spire2 (an isoform of Spire proteins on the vesicle membrane) and Rab11a (Fig. 1). Since the GTBM fragment of Spire binds to subdomain-1 of Myo5 GTD, and GTD can interact with and inhibit N-terminal motor head function, it is possible that Spire-GTBM can disrupt this head-tail interaction and release the motor head function. To test this hypothesis, we measured the actin-activated ATPase activity of Myo5b in the presence of Spire2-GTBM. As depicted in Fig. 2A, the addition of 8  $\mu$ M Spire2-GTBM stimulated the inhibited activity of Myo5b to approximately 1.8-fold under EGTA conditions.

We further characterized the Spire2-GTBM dependent actinactivated ATPase activity of Myo5b. In the presence of 200 mM KCl, Myo5b ATPase activity was activated by Spire2-GTBM with a maximal ATPase activity ( $V_{\rm max}$ ) of 1.40  $\pm$  0.24 head  $^{-1}$ s  $^{-1}$ , and an apparent affinity ( $K_m$ ) of 7.70  $\pm$  2.67  $\mu$ M (Fig. 2B). The maximal activated Myo5b activity by saturated Spire2-GTBM was  $\sim$ 2.6-fold higher than that in the absence of Spire2-GTBM (referred to as  $V_0$ , 0.89  $\pm$  0.04 head  $^{-1}$ s  $^{-1}$ ).

Another vesicular adaptor, Rab11a, weakly stimulated Myo5b activity (Fig. 2A), which is consistent with our previous work [15]. Considering Spire2-GTBM and Rab11a bind to subdomain-1 and 2 of Myo5 GTD, respectively. It is possible that Spire2 and Rab11a collaboratively regulate Myo5b motor function. We measured the actin-activated ATPase activity of Myo5b in the presence of Spire2 and Rab11a, we found that Spire2-GTBM and Rab11a substantially collaboratively stimulated the activity of Myo5b (Fig. 2A, the fourth column). The addition of 5  $\mu$ M Rab11a significantly increased the  $V_{\rm max}$  (2.70  $\pm$  0.25 head $^{-1}$ s $^{-1}$ ) and decreased the  $K_m$  (4.05  $\pm$  0.35  $\mu$ M) of Myo5b ATPase activity activated by Spire2-GTBM (Fig. 2B).

Next, we examined the effect of ionic strength on the activity of

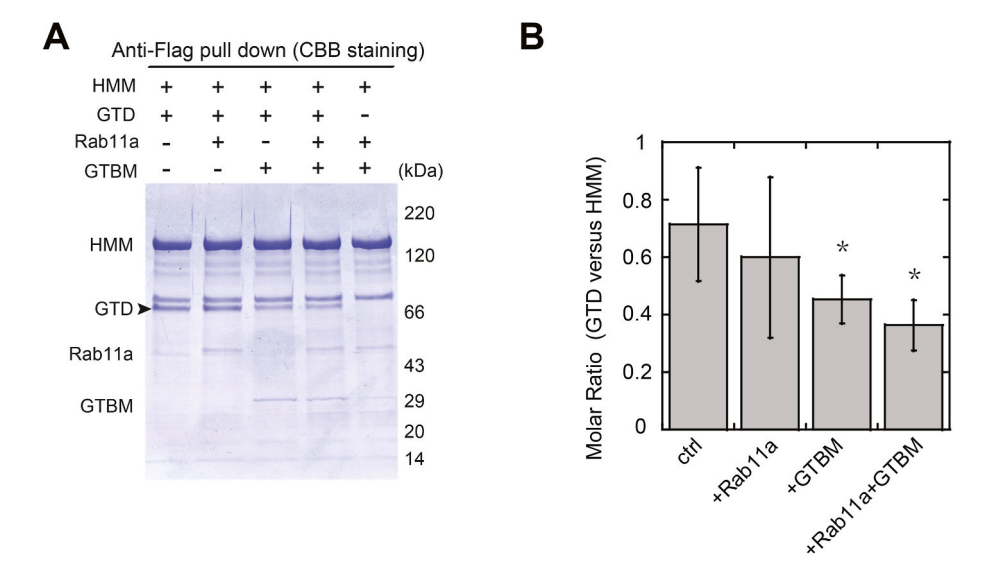


Fig. 3. Spire2-GTBM and Rab11a weakened the head-tail interaction of Myo5b. (A) Anti-FLAG pulldown of Myo5b-HMM with GTD in the absence or presence of Rab11a and Spire2-GTBM. The solution containing FLAG-tagged Myo5b-HMM, GST-tagged GTD and Rab11a or Spire2-GTBM was pulled down by anti-FLAG agarose, and the bound proteins were eluted by FLAG peptide. The eluted proteins were subjected to SDS-PAGE and Coomassie blue staining (for detail, see "Materials and methods" section). (B) The molar ratio of pulled down Myo5b-GTD *versus* Myo5b-HMM. The amounts of GTD and HMM pulled down were quantified based on their molecular masses using the ImageJ program. Values are mean  $\pm$  S.D. from four independent assays. Asterisk (\*, P < 0.05) indicates a statistically significant difference compared to the first column. (For interpretation of the references to colour in this figure legend, the reader is referred to the Web version of this article.)

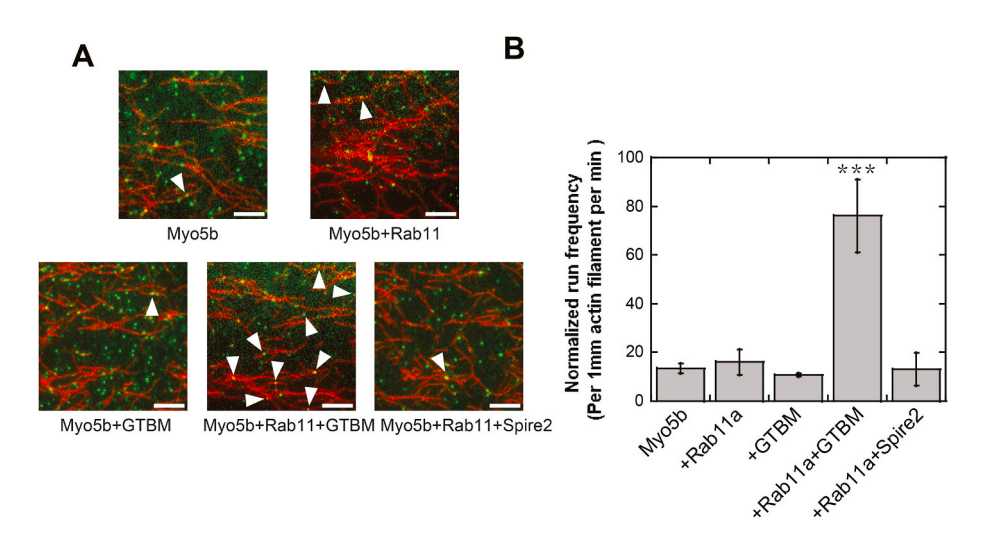


Fig. 4. Spire2 and Rab11a synergistically activated Myo5b motility activity. (A) Single-molecule imaging of Cy3B-labeled Myo5b molecules (green, indicated by arrowheads) moving along Alexa-488 labeled actin filaments (red) in the absence or presence of 1  $\mu$ M Spire2-GTBM and/or 5  $\mu$ M Rab11a. For clarity, only a part of the image (150  $\times$  150 pixels) is shown. Scale bars, 5  $\mu$ m. (B) Frequency of Cy3B-labeled Myo5b moving along Alexa 488-labeled actin filaments within a fixed time and area. The values are normalized to 1 mm length of actin filament per minute. Values are mean  $\pm$  S.D. from 3 to 5 different movies. Asterisks denote a statistically significant difference compared to the first column (\*\*\*\*, P < 0.001). (For interpretation of the references to colour in this figure legend, the reader is referred to the Web version of this article.)

Myo5b activated by Spire2-GTBM and Rab11a. As depicted in Fig. 2C, the Myo5b ATPase activity activated by 8  $\mu$ M Spire2-GTBM and/or 10  $\mu$ M Rab11a were highly dependent on ionic strength. The Myo5b ATPase activity activated by Spire2-GTBM or Rab11a reached its maximum at approximately 300 mM KCl, compared to the absence of these factors (Fig. 2C). In the presence of both Spire2-GTBM and Rab11a, the stimulated activity peaked at around 200 mM KCl, indicating that both Spire2-GTBM and Rab11a are required to activate Myo5b motor function under physiological ionic strength conditions (Fig. 2C). The stimulated activity of Myo5b in the presence of Spire2-GTBM and/or Rab11a at high ionic strength conditions (300–500 mM KCl) decreased, which may be caused by the disruption of interactions

between GTBM/Rab11a and GTD in such a high ionic strength solution.

# 3.2. Spire2 and Rab11a disrupt the head-tail interaction of Myo5b

To investigate whether Spire2-GTBM and Rab11a affect the head-tail interaction of Myo5b, we performed an anti-FLAG pulldown assay using FLAG-tagged Myo5b-HMM with GST-tagged Myo5b-GTD in the presence of Spire2-GTBM and/or Rab11a. The pulled down Myo5b-GTD was then analyzed by SDS-PAGE. As shown in Fig. 3, Rab11a and Spire2-GTBM individually reduced the amount of GTD pulled down with Myo5b-HMM. The amount of pulled down Myo5b-GTD substantially reduced upon the addition of both Spire2-GTBM and Rab11a. These

results suggest that the enhanced ATPase activity of Myo5b is due to the disruption of the Myo5b head-tail interaction.

## 3.3. Spire2 and Rab11a synergistically stimulate Myo5b motility activity

To further investigate the effects of Spire2-GTBM and Rab11a on Myo5b motor function, we performed a single-molecule motility assay of Myo5b. Cy3B-labeled Myo5b was mixed with 1 µM Spire2-GTBM and/or 5 µM Rab11a and then fluxed into an Alexa 488-labeled actin filaments-covered flow chamber. The movement of Cy3B-labeled Myo5b was recorded using a total internal reflection fluorescence (TIRF) microscope. As depicted in Fig. 4A and Movies S1-S5, only a few Cy3Blabeled Myo5b molecules moved on actin filaments in the absence of Spire2-GTBM and Rab11a. The addition of either Spire2-GTBM or Rab11a alone, or full-length Spire2 together with Rab11a, did not significantly increase the number of moving Myo5b molecules. However, upon the addition of both Spire2-GTBM and Rab11a, the number of Myo5b molecules moving increased 5.7-fold compared to that in the absence of Spire2-GTBM and Rab11a (Fig. 4B), indicating that both Spire2-GTBM and Rab11a are necessary to activate the motor motility activity of Myo5b.

#### 4. Discussion

The coupling of myosin motility and actin track assembly in vesicle long-distance transport has recently been discovered in some cells. In mouse oocytes, the membrane-associated Spire and Rab11a are indispensable for the Myo5b dependent long-distance transport. However, it is still unclear how Spire and Rab11a influence Myo5b activity during intracellular transport. In the present study, we demonstrate that Spire2-GTBM and Rab11a collaboratively regulate the ATPase and motility activity of Myo5b.

An important question is how the binding of Spire2-GTBM and Rab11a relieves the head-tail interaction and activates the motor function of Myo5b. Structural and biochemical evidence demonstrates that Spire2-GTBM and Rab11a bind to subdomain-1 and 2 of Myo5a-GTD, respectively, forming a GTD/Spire-GTBM/Rab11a ternary complex [18,28]. Interestingly, the Spire2-GTBM binding groove on the GTD surface is the binding region for a strand extending from the N-terminus of the neighboring GTD, which is essential for GTD dimer formation [18, 28-30]. On the other hand, the binding surface of Rab11a on subdomain-2 of GTD partially overlaps with the first calmodulin at the neck region of Myo5a [30]. Considering the high sequence similarity between Myo5a and Myo5b, the binding of Spire2-GTBM and Rab11a to the GTD may respectively disrupt the stable structure of the GTD dimer and the head-tail interaction of Myo5b, leading to the activation of Myo5b. In addition, one short fragment of melanophilin, GTBDP, which shares an overlapping binding site with Spire2-GTBM, can allosterically inhibit the head-GTD interaction of Myo5a [18,30,31], suggesting that allosteric regulation may also be involved in the activation of Myo5b. It should be noted that, in the present study, full-length Spire2 has little effect on the activation of Myo5b (Figs. 2A and 4B). To exclude the possibility of protein misfolding, we performed an actin polymerization assay in the presence of Spire2 proteins. Our data showed that the purified full-length Spire2 proteins significantly stimulated actin polymerization (Fig. S1), indicating the purified proteins are well-folded. Tittel and colleagues demonstrate that the N-terminal KIND domain of Spire2 strongly binds to the C-terminal FYVE-type domain [32], this intramolecular interaction may hinder the GTBM binding to Myo5b-GTD and subsequently affect the activation of Myo5b. Further research is needed to address this issue.

In addition to mouse oocytes, similar microfilament networks have also been observed in *Drosophila* and *Xenopus* oocytes [33–35]. Furthermore, several studies demonstrate that Myo5a, in synergy with Spire, is recruited to specific vesicles in melanocytes and HeLa cells [3,4, 36]. These findings suggest that specific vesicles, which recruit

molecular motor and actin nucleation factors, and perform long-distance movement along self-assemble microfilament mesh may be widely present in cells. Our work may provide a general explanation for this vesicle transport. However, further studies regarding the formation, function and intermolecular regulation of such multi-protein complexes are still necessary to improve our understanding of intracellular transport processes.

# CRediT authorship contribution statement

**Lin-Lin Yao:** Writing – original draft, Investigation, Formal analysis, Data curation, Conceptualization. **Wei-Dong Hou:** Validation, Investigation, Formal analysis, Data curation. **Yi Liang:** Investigation, Formal analysis. **Xiang-dong Li:** Writing – review & editing, Resources, Formal analysis. **Huan-Hong Ji:** Writing – review & editing, Project administration, Funding acquisition, Conceptualization.

#### **Declaration of competing interest**

The authors declare that they have no known competing financial interests or personal relationships that could have appeared to influence the work reported in this paper.

## Acknowledgements

This work was supported by the National Natural Science Foundation of China [grant number 32000486], Traditional Chinese Medicine Science and Technology Plan Project of Jiangxi Provincial Administration [grant number 2022B1012], and State Key Laboratory of Integrated Management of Pest Insects and Rodents [grant number IPM2110].

#### Appendix A. Supplementary data

Supplementary data to this article can be found online at https://doi.org/10.1016/j.bbrc.2024.149653.

# References

- [1] S. Pfender, V. Kuznetsov, S. Pleiser, E. Kerkhoff, M. Schuh, Spire-type actin nucleators cooperate with formin-2 to drive asymmetric oocyte division, Curr. Biol. 21 (2011) 955–960, https://doi.org/10.1016/j.cub.2011.04.029.
- [2] M. Schuh, An actin-dependent mechanism for long-range vesicle transport, Nat. Cell Biol. 13 (2011) 1431–1436, https://doi.org/10.1038/ncb2353.
- [3] R.D. Evans, C. Robinson, D.A Briggs, D.J Tooth, J.S Ramalho, M. Cantero, L. Montoliu, S. Patel, E.V Sviderskaya, A.N Hume, Myosin-va and dynamic actin oppose microtubules to drive long-range organelle transport, Curr. Biol. 15 (2014) 1743–1750, https://doi.org/10.1016/j.cub.2014.06.019.
- [4] N. Alzahofi, T. Welz, C.L. Robinson, E.L. Page, D.A. Briggs, A.K. Stainthorp, J. Reekes, D.A. Elbe, F. Straub, W.W. Kallemeijn, E.W. Tate, P.S. Goff, E. V. Sviderskaya, M. Cantero, L. Montoliu, F. Nedelec, A.K. Miles, M. Bailly, E. Kerkhoff, A.N. Hume, Rab27a co-ordinates actin-dependent transport by controlling organelle-associated motors and track assembly proteins, Nat. Commun. 11 (2020) 3495, https://doi.org/10.1038/s41467-020-17212-6.
- [5] Z. Holubcová, G. Howard, M. Schuh, Vesicles modulate an actin network for asymmetric spindle positioning, Nat. Cell Biol. 15 (2013) 937–947, https://doi. org/10.1038/ncb2802.
- [6] S. Watanabe, K. Mabuchi, R. Ikebe, M. Ikebe, Mechanoenzymatic characterization of human myosin Vb, Biochemistry-Us 45 (2006) 2729–2738, https://doi.org/ 10.1021/bi051682b.
- [7] L. Gardini, S.M. Heissler, C. Arbore, Y. Yang, J.R. Sellers, F.S. Pavone, M. Capitanio, Dissecting myosin-5B mechanosensitivity and calcium regulation at the single molecule level, Nat. Commun. 9 (2018) 2844, https://doi.org/10.1038/ s41467-018-05251-z.
- [8] M. Ikebe, Regulation of the function of mammalian myosin and its conformational change, Biochem. Biophys. Res. Commun. 369 (2008) 157–164, https://doi.org/ 10.1016/j.bbrc.2008.01.057.
- [9] J.R. Sellers, K. Thirumurugan, T. Sakamoto, J.R. Hammer, P.J. Knight, Calcium and cargoes as regulators of myosin 5a activity, Biochem. Biophys. Res. Commun. 369 (2008) 176–181
- [10] K.M. Trybus, Myosin V from head to tail, Cell. Mol. Life Sci. 65 (2008) 1378–1389, https://doi.org/10.1016/j.bbrc.2007.11.109.
- [11] N. Zhang, L.L. Yao, X.D. Li, Regulation of class V myosin, Cell. Mol. Life Sci. 75 (2018) 261–273, https://doi.org/10.1007/s00018-017-2599-5.

- [12] S.L. Reck-Peterson, D.W.P. Jr, M.S. Mooseker, J.A Mercer, Class V myosins, Biochim. Biophys. Acta Mol. Cell Res. 1 (2000) 36–51, https://doi.org/10.1016/ s0167-4889(00)00007-0.
- [13] K. Thirumurugan, T. Sakamoto, J.R. Hammer, J.R. Sellers, P.J. Knight, The cargo-binding domain regulates structure and activity of myosin 5, Nature 442 (2006) 212–215, https://doi.org/10.1038/nature04865.
- [14] Z. Wang, J.G. Edwards, N. Riley, D.J. Provance, R. Karcher, X.D. Li, I.G. Davison, M. Ikebe, J.A. Mercer, J.A. Kauer, M.D. Ehlers, Myosin Vb mobilizes recycling endosomes and AMPA receptors for postsynaptic plasticity, Cell 135 (2008) 535–548, https://doi.org/10.1016/j.cell.2008.09.057.
- [15] H. Ji, L. Yao, C. Liu, X. Li, Regulation of myosin-5b by Rab11a and the Rab11 family interacting protein 2, Biosci. Rep. 39 (2019), https://doi.org/10.1042/BSR20181252. BSR20181252.
- [16] E. Kerkhoff, Actin dynamics at intracellular membranes: the Spir/formin nucleator complex, Eur. J. Cell Biol. 90 (2011) 922–925, https://doi.org/10.1016/j. eich 2010 10 011
- [17] S. Dietrich, S. Weiß, S. Pleiser, E. Kerkhoff, Structural and functional insights into the Spir/formin actin nucleator complex, Biol. Chem. 394 (2013) 1649–1660, https://doi.org/10.1515/hsz-2013-0176.
- [18] O. Pylypenko, T. Welz, J. Tittel, M. Kollmar, F. Chardon, G. Malherbe, S. Weiss, C.I. L. Michel, A. Samol-Wolf, A.T. Grasskamp, A. Hume, B. Goud, B. Baron, P. England, M.A. Titus, P. Schwille, T. Weidemann, A. Houdusse, E. Kerkhoff, Coordinated recruitment of Spir actin nucleators and myosin V motors to Rab11 vesicle membranes, Elife 5 (2016) e17523, https://doi.org/10.7554/eLife.17523.
- [19] J.A. Spudich, S. Watt, The regulation of rabbit skeletal muscle contraction. I. Biochemical studies of the interaction of the tropomyosin-troponin complex with actin and the proteolytic fragments of myosin, J. Biol. Chem. 246 (1971) 4866–4871, https://doi.org/10.1016/S0021-9258(18)62016-2.
- [20] X. Li, K. Mabuchi, R. Ikebe, M. Ikebe, Ca<sup>2+</sup>-induced activation of ATPase activity of myosin Va is accompanied with a large conformational change, Biochem. Biophys. Res. Commun. 315 (2004) 538–545, https://doi.org/10.1016/j.bbrc.2004.01.084.
- [21] X. Li, H.S. Jung, K. Mabuchi, R. Craig, M. Ikebe, The globular tail domain of myosin Va functions as an inhibitor of the myosin Va motor, J. Biol. Chem. 281 (2006) 21789–21798, https://doi.org/10.1074/jbc.M602957200.
- [22] Z. Lu, M. Shen, Y. Cao, H. Zhang, L. Yao, X. Li, Calmodulin bound to the first IQ motif is responsible for calcium-dependent regulation of myosin 5a, J. Biol. Chem. 287 (2012) 16530–16540, https://doi.org/10.1074/jbc.M112.343079.
- [23] X.D. Li, H.S. Jung, Q. Wang, R. Ikebe, R. Craig, M. Ikebe, The globular tail domain puts on the brake to stop the ATPase cycle of myosin Va, Proc. Natl. Acad. Sci. U. S. A. 105 (2008) 1140–1145, https://doi.org/10.1073/pnas.0709741105.
- [24] Y. Sun, O. Sato, F. Ruhnow, M.E. Arsenault, M. Ikebe, Y.E. Goldman, Single-molecule stepping and structural dynamics of myosin X, Nat. Struct. Mol. Biol. 17 (2010) 485–491, https://doi.org/10.1038/nsmb.1785.

- [25] Q. Cao, N. Zhang, R. Zhou, L. Yao, X. Li, The cargo adaptor proteins RILPL2 and melanophilin co-regulate myosin-5a motor activity, J. Biol. Chem. 294 (2019) 11333–11341, https://doi.org/10.1074/jbc.RA119.007384.
- [26] M. Shen, N. Zhang, S. Zheng, W. Zhang, H. Zhang, Z. Lu, Q.P. Su, Y. Sun, K. Ye, X. Li, Calmodulin in complex with the first IQ motif of myosin-5a functions as an intact calcium sensor, Proc. Natl. Acad. Sci. U. S. A. 113 (2016) E5812–E5820, https://doi.org/10.1073/pnas.1607702113.
- [27] D. V. Trivedi, J.M. Muretta, A.M. Swenson, J.P. Davis, D.D. Thomas, C.M. Yengo, Direct measurements of the coordination of lever arm swing and the catalytic cycle in myosin V, Proc. Natl. Acad. Sci. U. S. A. 112 (2015) 14593–14598, https://doi. org/10.1073/onas.1517566112.
- [28] O. Pylypenko, W. Attanda, C. Gauquelin, M. Lahmani, D. Coulibaly, B. Baron, S. Hoos, M.A. Titus, P. England, A.M. Houdusse, Structural basis of myosin V Rab GTPase-dependent cargo recognition, Proc. Natl. Acad. Sci. U. S. A. 110 (2013) 20443–20448, https://doi.org/10.1073/pnas.1314329110.
- [29] W. Zhang, L. Yao, X. Li, The globular tail domain of myosin-5a functions as a dimer in regulating the motor activity, J. Biol. Chem. 291 (2016) 13571–13579, https://doi.org/10.1074/jbc.M116.724328.
- [30] F. Niu, Y. Liu, K. Sun, S. Xu, J. Dong, C. Yu, K. Yan, Z. Wei, Autoinhibition and activation mechanisms revealed by the triangular-shaped structure of myosin Va, Sci. Adv. 8 (2022) eadd4187, https://doi.org/10.1126/sciadv.add4187.
- [31] L. Yao, Q. Cao, H. Zhang, J. Zhang, Y. Cao, X. Li, Melanophilin stimulates myosin-5a motor function by allosterically inhibiting the interaction between the head and tail of myosin-5a, Sci Rep-Uk 5 (2015) 10874, https://doi.org/10.1038/srep10874.
- [32] J. Tittel, T. Welz, A. Czogalla, S. Dietrich, A. Samol-Wolf, M. Schulte, P. Schwille, T. Weidemann, E. Kerkhoff, Membrane targeting of the Spir-formin actin nucleator complex requires a sequential handshake of polar interactions, J. Biol. Chem. 290 (2015) 6428–6444, https://doi.org/10.1074/jbc.M114.602672.
- [33] J. Taunton, B.A. Rowning, M.L. Coughlin, M. Wu, R.T. Moon, T.J. Mitchison, C. A. Larabell, Actin-dependent propulsion of endosomes and lysosomes by recruitment of N-WASP, J. Cell Biol. 148 (2000) 519–530, https://doi.org/10.1083/jcb.148.3.519.
- [34] K. Dahlgaard, A.A. Raposo, T. Niccoli, D. St Johnston, Capu and Spire assemble a cytoplasmic actin mesh that maintains microtubule organization in the Drosophila oocyte, Dev. Cell 13 (2007) 539–553, https://doi.org/10.1016/j. devcel.2007.09.003.
- [35] C.M. Field, M. Wühr, G.A. Anderson, H.Y. Kueh, D. Strickland, T.J. Mitchison, Actin behavior in bulk cytoplasm is cell cycle regulated in early vertebrate embryos, J. Cell Sci. 124 (2011) 2086–2095, https://doi.org/10.1242/jcs.082263.
- [36] T. Welz, E. Kerkhoff, Exploring the iceberg: prospects of coordinated myosinV and actin assembly functions in transport processes, Small GTPases 10 (2019) 111–121, https://doi.org/10.1080/21541248.2017.1281863.